



# Development of a finite element groundwater flow model to test drainage management strategies for the expansion of the Dareh-Zar open pit mine, Iran

Hossein Parsasadr<sup>1</sup> · Syed Mustafa<sup>1</sup> · Mohsen Golian<sup>2</sup> · Victor Bense<sup>1</sup>

Received: 31 August 2023 / Accepted: 9 April 2024  
© The Author(s) 2024

## Abstract

A finite-element groundwater flow model was developed for the expanding Dareh-Zar open pit mine in southern Iran, to simulate groundwater inflow into the excavation and mine wall pore pressure dynamics. The model was used to test the effectiveness of implementing different drainage management strategies to reduce groundwater inflow rates and mine wall pore pressures, including abstraction wells and horizontal drains. Model predictions suggest the implementation of abstraction wells will reduce groundwater inflow rates by 75% during the first 12 years of mining and 50% during the subsequent 5 years relative to a ‘no drainage’ management scenario, with further reductions in groundwater inflow achieved through horizontal drain installation. Furthermore, the installation of horizontal drains was found to be necessary to reduce mine-wall pore pressures from destabilizing the mine walls. Groundwater management of the decommissioned pit mine was also evaluated, with simulation results suggesting that backfilling the excavation would restore the groundwater level within the open pit mine region to ~2,442 m above sea level, representing a net restoration of ~204 m relative to the water table prior to mine closure.

**Keywords** Groundwater modeling · Iran · Dynamic mesh · Mining · Dewatering

## Introduction

Excavation of open pit mines below the water table can result in groundwater inflow into the mining pit (Bozan et al. 2022). Groundwater inflow into open pit mines can cause significant impacts to the environment (McCullough and Lund 2006) and provides technical and operational challenges to mining, associated with increased costs of blasting (Zago et al. 2020), and disruption to loading and transportation (Taherkhani and Doostmohammadi 2015). In addition, steep hydraulic gradients can develop across the highwalls of open-pit mines, increasing the pore pressure of mine walls and resulting in shear stress, instability, and potential failure

(Kolapo et al. 2022). Therefore, estimation of the groundwater inflow rate into an open pit mine is crucial for designing effective drainage systems and predicting changes in the pore pressure distribution of the mine walls to ensure the stability and safety of the mine operations.

Numerous researchers have dedicated their efforts to predicting groundwater inflow into open pit mines (Atkinson et al. 2010; Azrag et al. 1998; Cotesta et al. 2020; Robins et al. 2005; and Rózkowski et al. 2021), as it is crucial for the design and optimization of drainage systems (Polomčić and Bajić 2015). Previous studies have employed various methodologies, including finite difference models such as SEEP/W (Bahrami et al. 2014) and MODFLOW (Fernández-Álvarez et al. 2016; Jiang et al. 2013), as well as analytical solutions (Aryafar et al. 2007; Li et al. 2014) and machine learning algorithms (Bahrami et al. 2016).

MODFLOW (Harbaugh 2005) and FEFLOW (Diersch 2013) are conventional groundwater modeling codes based on the equivalent porous medium (EPM) approach, that are frequently used to simulate groundwater flow in fractured porous media. MODFLOW is commonly employed for simulating groundwater flow in orthogonal fracture

✉ Hossein Parsasadr  
hossein.parsasadr@wur.nl

<sup>1</sup> Hydrology and Environmental Hydraulics Group, Wageningen University & Research, Wageningen, the Netherlands

<sup>2</sup> Tehran Science and Research Branch, Islamic Azad University, Tehran, Iran

systems, whereas FEFLOW is often preferred for modeling irregular fracture systems (Kresic and Panday 2018; Rivera 2007).

Despite the utility of MODFLOW and FEFLOW, these models possess inherent limitations that hinder their effectiveness for groundwater modeling in mining environments. This study accounts for the specialized characteristics unique to mining operations. This includes the use of a dynamic mesh to account for open pit excavation and alterations in hydrogeologic properties surrounding mines, resulting from stress relief due to overburden removal and blast-induced damage. Specifically, a zone of relaxation (ZOR) has been developed as a key factor influencing the simulation of groundwater inflow into the open pit mine. Additionally, this study examines the formation of the pit lake after mining and dewatering ends as well as the recovery of the groundwater system after closure or backfilling. Furthermore, simulation of seepage faces was used as a validation process in this study, involving the simulation of seepage faces, serving as a verification factor to ensure the reliability of the model.

For this study, a groundwater finite element model (FEM) was used to predict groundwater inflow into the Dareh-Zar open pit mine. The advantages of FEM approaches include the capability to handle complex boundary conditions, accommodate high-resolution spatial and temporal dynamics, and incorporate heterogeneous subsurface properties.

The Dareh-Zar open-pit copper mine has been strip-mined and extracted for almost two decades, and the main mining process is carried out below the water table. Currently, seepage faces are present in the Dareh-Zar mine, ranging from 2,500 m above sea level (m ASL) in the current pit floor to ~2,563 m ASL along the eastern mine wall. Groundwater discharge has formed a sizable pond in the southern section of the pit floor, measuring ~290 m<sup>2</sup> in area and exceeding a depth of 10 m. Additionally, smaller ponds have emerged near the seepage faces, commonly used as water sources for spraying mine berms and benches to reduce the dispersion of airborne respirable dust. The mine development plan projects the pit floor level will reach a depth of 2,230 m ASL within the next 17 years, equivalent to 300 m below the water table.

This report aims to predict the groundwater inflow rate to the Dareh-Zar mine pit through numerical modeling using a 3D groundwater FEM. The specific objectives include: (1) developing and evaluating the performance of the FEM specifically for the Dareh-Zar mine area, (2) assessing various management scenarios to identify the most suitable option for designing an optimized drainage system, and (3) determining the distribution of pore pressure in the pit walls over different time periods in order to evaluate the most effective operational management system for the sustainable development of the Dareh-Zar copper mine.

## Materials and methods

### Geological and Hydrological setting

The Dareh-Zar copper mine is located 170 km southwest of Kerman Province and 10 km south of the Sarcheshmeh copper mine (N 29°52'60" and E 55°54'20") (Fig. 1). The most significant porphyry copper deposits in Iran, including the Dareh-Zar mine, lie in a tectonically active zone on the south of Urumieh-Dokhtar Magmatic Assemblage (UDMA) and the central part of Dehaj-Sardouieh strip, which is the most important metallogenic belt in Iran (Movahednia et al. 2022). The study area is characterized by a diverse range of geological units (Fig. 1). The oldest units in the area are of Eocene age, represented by pyroclastic and volcanic rocks, and consist of tuff and tuffite, lithic tuff, crystal tuff, and volcanic rocks with acidic to intermediate composition and, less frequently, intermediate to basic composition. Overlying the Eocene volcanics are younger, Quaternary deposits consisting of unconsolidated sediments of gravel, sand, and silt textures. The Dareh-Zar study area is highly altered and significantly faulted, resulting in a reduction in the mechanical strength of the rock mass (Parizi and Samani 2014; Mali et al. 2022). The Dareh-Zar faults primarily exhibit E–W and N–S orientations, with subvertical dip angles. Notably, the E–W faults are older than the N–S faults. The formation of fractures within the study area is primarily attributed to the development of contraction joints during the crystallization of magma, tectonic activity, and weathering processes, resulting in enhanced permeability of the rock mass, facilitating groundwater flow and discharge into the open mine pit (KMP 2020).

The study area experiences an arid climate, characterized by low annual precipitation and high evapotranspiration rates. Precipitation is highly seasonal, with the majority of the annual rainfall occurring in the winter months as high-intensity storm events, whereas summer months receive minimal rainfall. The Dareh-Zar open pit mine receives an average annual rainfall of 312 mm, while the mean annual precipitation within the model domain ranges from 225 to 378 mm (KMP 2019). Assuming a recharge rate of ~10–15% of annual rainfall, the average groundwater recharge resulting from precipitation exceeds 40 mm/year. The average annual temperature is 13.4 °C, ranging from 3.1 °C in February to 21.3 °C in July.

Seasonal fluctuations in groundwater levels, monitored monthly using a network of 20 observation wells, are observed in the study area (Fig. 1). These data indicate groundwater flow generally follows a north–south direction, in accordance with the regional topography and geology. However, a significant shift in the hydraulic gradient

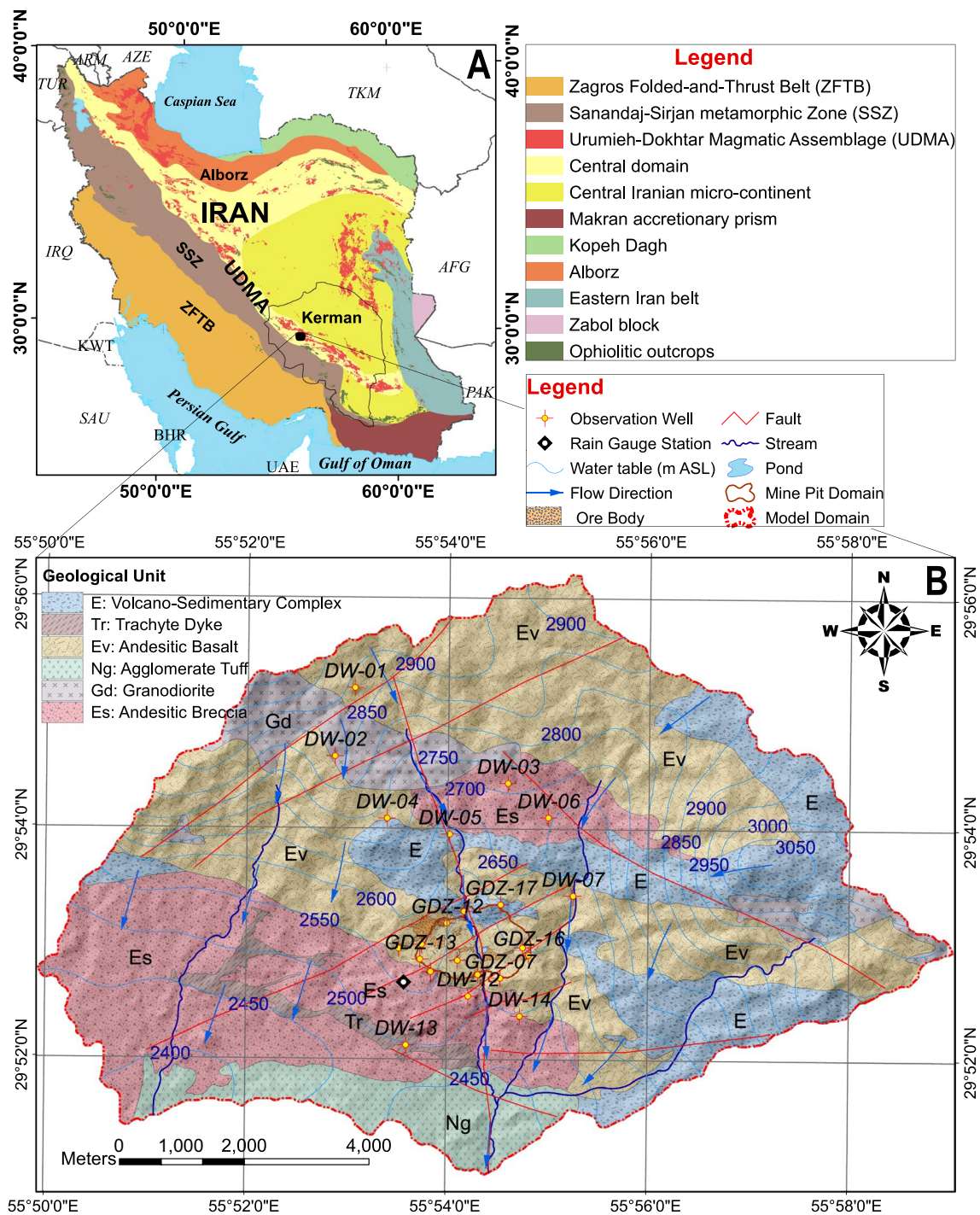


**Fig. 1** **A** Location of Dareh-Zar open pit mine in Iran, featuring major bedrock lithologies, and **B** detailed study area map showing contoured observations of groundwater level and groundwater flow directions for March 2017

is present adjacent to the mine pit, resulting in flow from the east and west walls towards the pit (Fig. 1). As a result of the open pit mine excavation, groundwater levels exceed the pit floor and the western mine wall, whereas the maximum depth of groundwater adjacent to the east wall is ~60 m below ground level.

As elsewhere (Bense et al. 2013), faults play a significant role in controlling surface water and groundwater flows in the study area. The Dareh-Zar River follows a north–south direction along a major fault, while also serving as a channel for groundwater drainage towards the mine area (Fig. 1). The hydraulic conductivity and groundwater flow systems

of hard rock aquifers are primarily governed by the spatial distribution of fractures, with petrographic attributes having a negligible impact on these properties (Krásný and Sharp 2007). Although the stress induced by the swelling of minerals such as olivine and pyroxene mainly in mafic and ultramafic rocks such as peridotites (Renard 2021; Sharp 2014) and biotite in plutonic and metamorphic rocks (Dewandel et al. 2017; Lachassagne et al. 2021) can generate fractures and accelerate the weathering process of the rock mass.

### Conceptual and numerical model development

This study constructed a numerical model using the MINEDW code, developed by Itasca Denver, Inc. (2023), a specialized three-dimensional (3D) finite-element groundwater modeling code designed explicitly for mining environments. The MINEDW code is based on the FEMFLOW3D algorithm (Durbin and Bond 1998), which was specifically developed to meet the needs of mine management (Azrag et al. 1998). One of the key features of MINEDW is the possibility to simulate the progressive excavation of an open pit by modifying the elevation of the nodes affected by mining over time. MINEDW can also efficiently simulate the formation of a zone of relaxation (ZOR) around a pit excavation or underground mining operation through time according to the mining schedule, where rock hydraulic properties are altered by open pit excavation or block cave mining. Additionally, the code includes a function for simulating backfill, which is commonly added to excavations and has different hydraulic properties than in-situ material. Finally, MINEDW includes a function for simulating pit lake development after the cessation of open pit mining (Ugoretz 2015).

The present study simulated the groundwater inflow rate to the Dareh-Zar open pit mine during mine operation and post-closure stages at the regional scale. For this purpose, the fractured hard rock aquifer in the study area was conceptualized using Esri's ArcGIS Pro and converted into a multilayered grid within MINEDW software. The conceptual groundwater model was then converted into a numerical model within MINEDW, which was calibrated to the observed head in both steady-state and transient modes. The model was then validated and recalibrated by comparing the simulated and observed seepage faces in the mine pit. A sensitivity analysis was conducted to assess uncertainty within the model input parameters. The validated numerical model was utilized for scenario modeling. The numerical modeling workflow is shown in Fig. 2.

### Model domain and boundary condition

To develop a groundwater conceptual model for the Dareh-Zar mine area, the geometry of the surrounding aquifer was determined and differentiated from adjacent aquifers using

hydraulic physical boundaries. Physical hydrological features that are known to control groundwater flow directions such as lakes, aquitards, and watershed divides were represented as boundary conditions (Wels et al. 2012). The catchment divides were assumed to be no-flow boundaries given the predominance of hard rock aquifers and an absence of observable karst features (Kollet and Maxwell 2008). Consequently, it is posited that the hydrological and hydrogeological catchments in this region are congruent; however, it is crucial to consider a sufficient distance when setting the boundaries of the model to ensure that the simulation of both present and future stresses is performed with high accuracy and devoid of any artificial boundary effects (Rossman et al. 2018). A catchment-scale modeling approach has been utilized in many studies to predict groundwater inflow into excavations, including underground and surface mines (Colombo et al. 2017; Gholizadeh et al. 2020; Golian et al. 2021, 2020, 2018; Yang et al. 2009).

The Dareh-Zar mine is situated across the catchment divide of the Goein and Dareh-Zar Rivers. The catchment borders were considered to be no-flow boundaries, except for the southern borders where the outflowing rivers were represented as constant head boundaries. The hydraulic head of these boundaries was assumed to be equivalent to the free surface water level of the corresponding rivers (Fig. 3). In the steady-state simulation, the initial head was defined as a constant value, determined by the average observation head during the steady-state modeling period within the model domain. The hydraulic heads obtained from the steady-state simulation results were subsequently utilized as the initial conditions for the transient simulation.

### Discretization

A feasible approach for simulating large-scale groundwater flow in rock masses involves the implementation of the equivalent porous medium (EPM) modeling approach (Scanlon et al. 2003). The EPM approach can minimize aquifer anisotropy induced by fractures in hard rocks at a sufficiently large scale (Surinaidu et al. 2014). Nevertheless, it is essential to model any significant fracture or fault zones using a layered modeling approach; therefore, finer discretization along fault zones, rivers, mining areas, and important hydrogeologic units may be necessary. In the present study, a two-dimensional (2D) finite element mesh was generated utilizing Rhino and Grasshopper software (Davidson 2021). The resulting mesh was then imported into MINEDW, where additional layers were incorporated to transform it into a 3D mesh. In the generated mesh, the model boundary, mine pit, and transition zone were distinguished from each other, with the mine pit featuring the finest element discretization. Similarly, the element sizes in the transition zone are discretized at an intermediate level between those in the mine pit and the

**Fig. 2** The workflow for developing the Dareh-Zar open pit mine groundwater model development

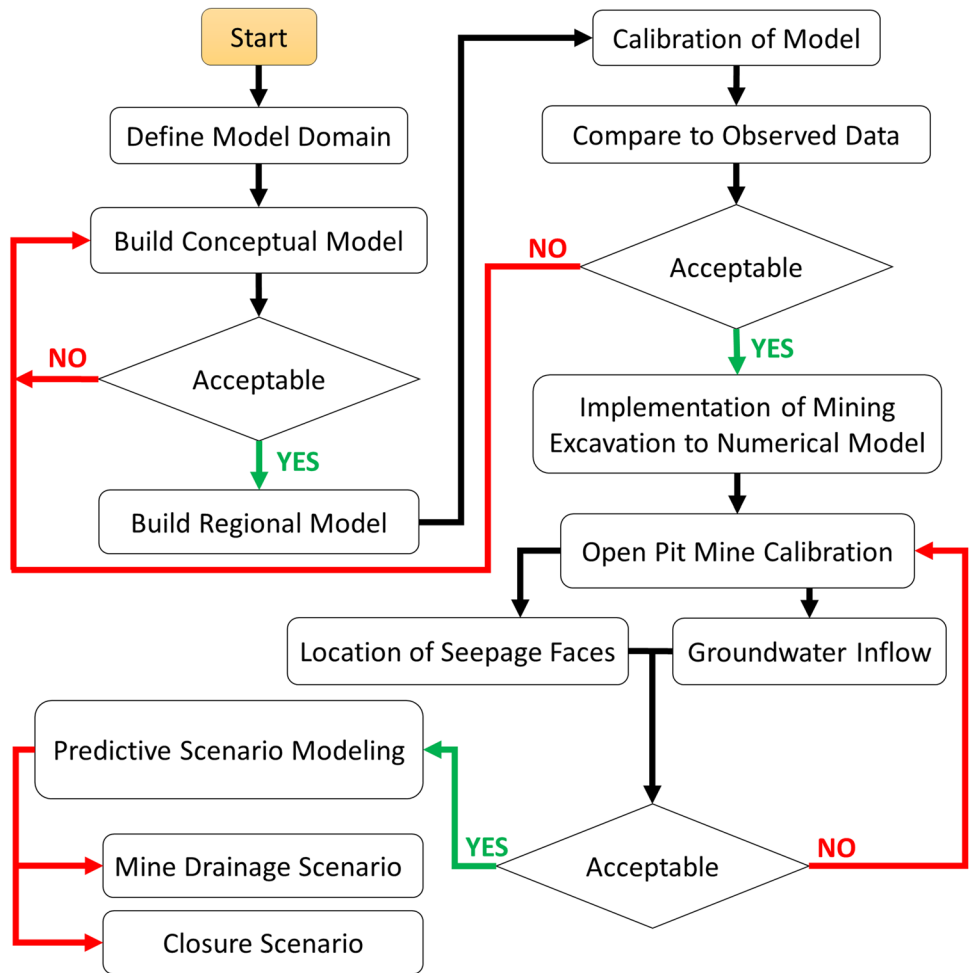
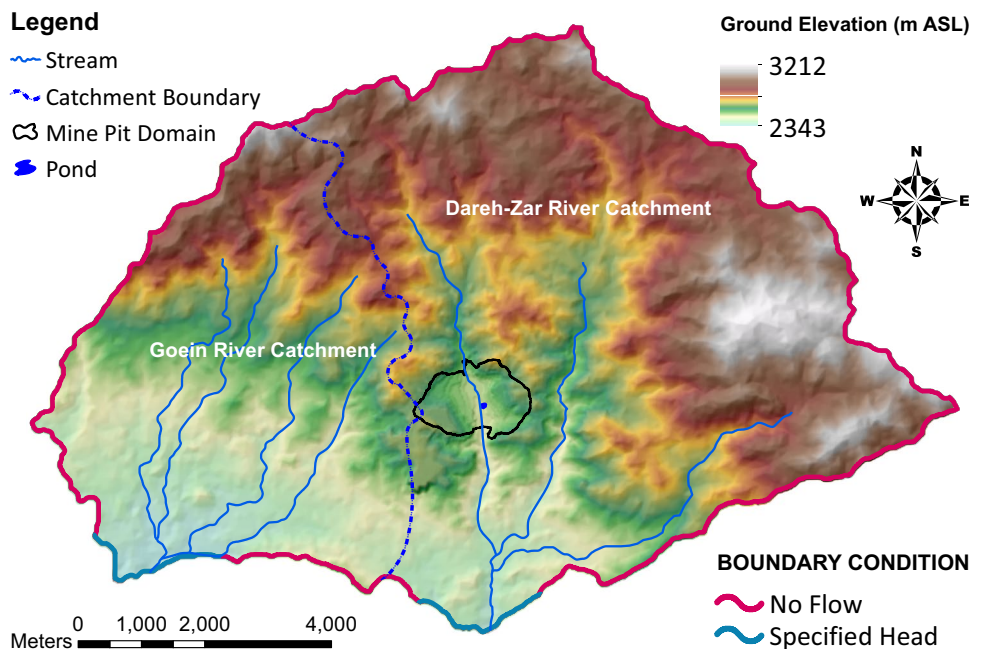


**Fig. 3** Model domain and boundary conditions of Dareh-Zar open pit mine groundwater model



model range. For this study, the transition zone was defined as a buffer region  $\sim 1$  km in width encircling the periphery of the open-pit mining site. The use of an intermediate mesh size in the transition zone is helpful in representing the gradual changes in these properties and avoiding abrupt changes that may cause numerical instability or inaccurate results (Holm and Langtangen 1999).

The methodology used for discretization in numerical modeling has a significant impact on predicting inflow and the water-table geometry around excavations, whether they are open pit or underground. Errors in estimating the seepage face height can introduce significant inaccuracies in predicted inflows and pore-pressure distribution, as this height affects both lateral inflow and the water-table elevation behind the mine walls. Therefore, to achieve accurate predictions of radial flow towards an excavation, it is crucial to use small logarithmic grid spacing in both horizontal and vertical directions in addition to finer discretization in the contact zone and faults. In this way, the pinch-out technique was utilized to partition the upper layer into eight strata, spanning from 5 to 40 m, while the middle layer was divided into eleven strata ranging from 40 to 100 m. The lowermost layer, on the other hand, maintained a uniform thickness of 500 m. Consequently, a progressive diminution in layer thickness from the base to the surface of the mesh was achieved. The top of the grid was defined as the ground surface elevation, based on ASTER GDEM (Tachikawa et al. 2011) and 1:1000 topographic map (NICICO 2017) of the mining area, and the grid bottom was defined

at 1,500 m ASL. Figure 4 illustrates the 3D mesh structure of the numerical model for the Dareh-Zar mine area.

### Hydrostratigraphic model

Numerical groundwater modeling requires the development of a hydrostratigraphic model (HSM), which simplifies the complex geological architecture of the study area (Barfod et al. 2018; Hudon-Gagnon et al. 2015). The HSM is focused on the identification and characterization of surface and subsurface geological units, primarily based on their hydrogeological properties (Allen et al. 2008), and is validated by analyzing lithological data, characterizing geological formations, and determining their physical properties (Giudici et al. 2012). A HSM was established by first identifying the geologic formations and fault distribution within the study area, based on the geological map, and subsequently simplifying the information as necessary. The geological framework of the region was taken into account, with each rock unit and fractured fault zone delineated as an individual hydrostratigraphic unit (HSU). Fracture and fault zones were identified and delineated using a comprehensive dataset encompassing field observations, field tests, geotechnical borehole data, and geological maps, enabling a more detailed representation of the heterogeneity of the aquifer. Forty HSUs were incorporated, with 13 specifically representing crushed and faulted zones; additionally, the geological block model of the Dareh-Zar copper porphyry deposit, which characterizes the geometrical properties of

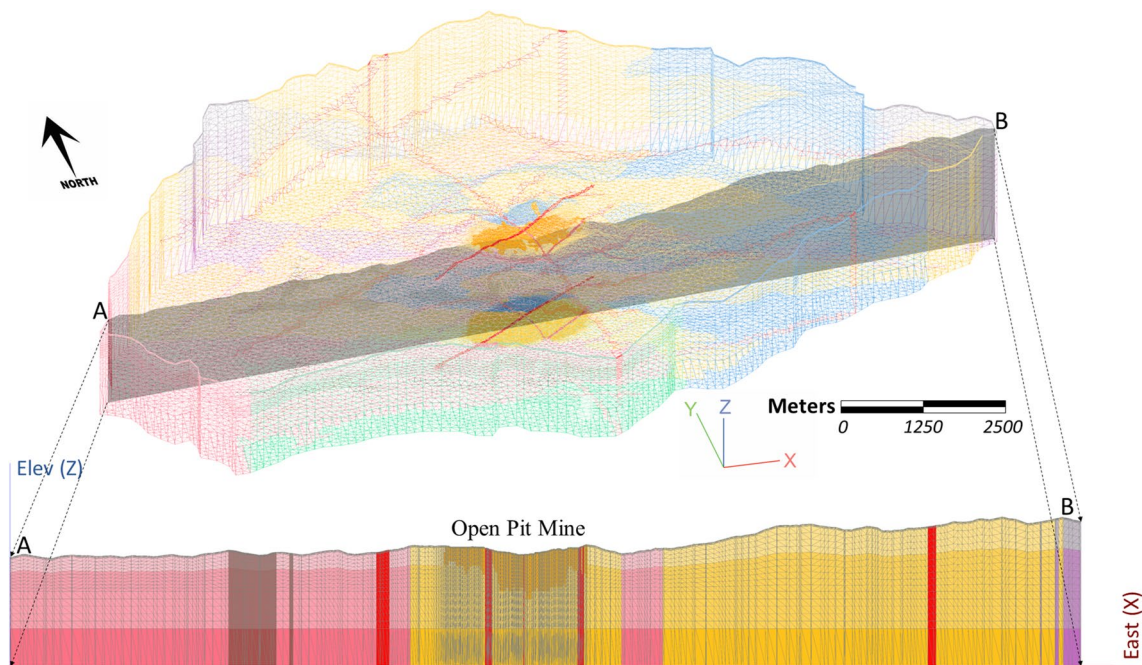


Fig. 4 3D mesh structure of the numerical model for Dareh-Zar open pit mine

the ore body, was developed using borehole data and was incorporated as an individual HSU in the HSM. Based on the correlation between rock mass permeability and rock quality designation (RQD) reported in previous studies (Cha et al. 2006; El-Naqa 2001; Jiang et al. 2009; Piscopo et al. 2018; Qureshi et al. 2014), the geotechnical borehole data was used to estimate the hydraulic properties of rock units and the separation of HSUs with respect to depth. Figure 5 presents the 3D hydrostratigraphy model of the studied area.

**Hydraulic Properties**

In this study, the zonation of HSUs in the model domain was determined from the geological map (Omaljev and Isailović 1969; Fig. 1). The predominant outcropping lithology of the Dareh-Zar study area comprises igneous rocks. Groundwater flow in fractured igneous rocks, formed by a combination of lithological conditions, local and regional geomechanical processes, and weathering (Shapiro et al. 2015), is primarily controlled by complex networks of fractures varying in orientation and extent. Therefore, the variation in hydraulic conductivity can be significant.

The initial hydraulic conductivity of the various HSUs was estimated by conducting pumping and airlift tests in the study area, which resulted in a wide range of values spanning from  $1 \times 10^{-2}$  to 3.6 m/day (SRK 2018). Higher values, exceeding 1 m/day, were primarily attributed to the fault zone ('crushed' unit in the model), consistent with the

higher frequency of seepage faces observed within these regions. Although there is some variation in hydraulic conductivity values among different igneous and metamorphic units, no clear distinction was determined between them (as shown in Fig. 6). It is worth noting that high hydraulic conductivity values indicate the presence of fractures within the rock, while low values represent relatively less fractured jointed rock masses.

Accurate determination of specific storage is crucial for reliable groundwater modeling in unsteady state conditions (Folnagy et al. 2013). Specific storage quantifies the ability of the aquifer to store water under varying hydrologic conditions. Inaccurate estimation of specific storage can result in flawed groundwater models, leading to inaccurate predictions of transient water flow and storage in the aquifer (Kuang et al. 2020). Based on the results of the pumping tests, the HSUs in the investigated area exhibit a range of storage coefficients over one order of magnitude, with the lowest recorded value being  $5 \times 10^{-4}$  and the highest being  $4 \times 10^{-3}$  (Sahraei Parizi and Samani 2013). The groundwater level in the study area exhibits a rapid response to seasonal precipitation, as evidenced by the groundwater hydrograph presented in Fig. 7. Consequently, the storage coefficient of the aquifer can be estimated by analyzing the groundwater hydrograph and utilizing the water-table fluctuation (WTF) method proposed by Seiler and Gat (2007). This method is particularly effective for estimating the storage coefficient of large-scale aquifers in semiarid regions (Wang et al. 2013;

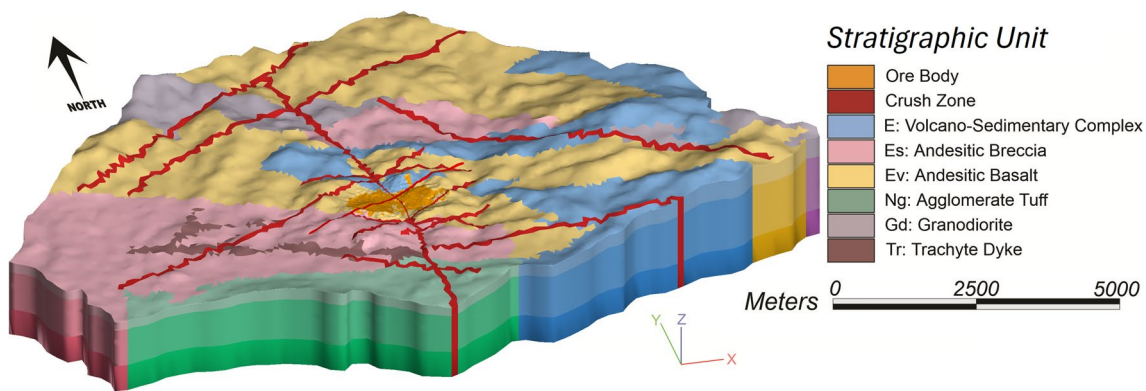


**Fig. 5** 3D hydrostratigraphy model for the Dareh-Zar open pit mine

**Fig. 6** Comparison of the measured ranges of hydraulic conductivity (*K*) across different hydrogeological units within the Dareh-Zar study area after Atkinson (2000), red lines indicate geometric means

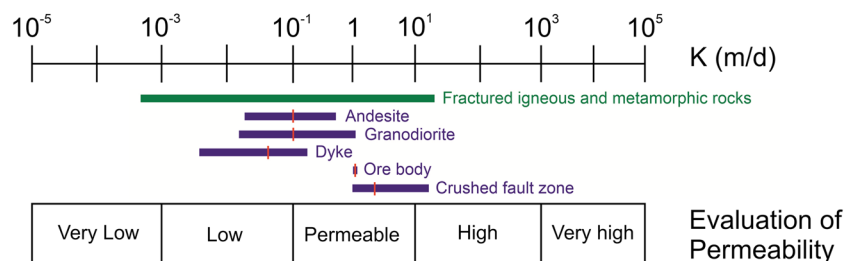
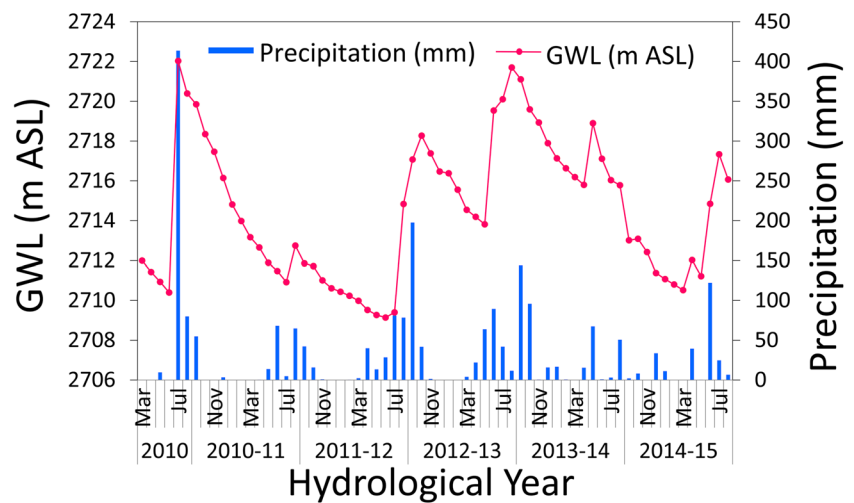


**Fig. 7** Response of groundwater level (GWL) hydrograph to precipitation (March 2010–August 2015)



Xu and Beekman 2019). Considering the range of rainfall infiltration into the groundwater body in the study area (10–15%) as reported by SRK (2018), the estimated average storage coefficient of the aquifer using the WTF method is consistent with the maximum value of the storage coefficient calculated by the pumping test method.

### Groundwater recharge

Spatial variation in groundwater recharge can be attributed to various factors such as geology, geomorphology, drainage density, lineament density, rock outcrops, topsoil, slope, precipitation, and land use (Sashikkumar et al. 2017). However, in the current study area, geology, geomorphology, and land use are similar, and soil cover is limited to areas adjacent to streams; therefore, the distribution of groundwater recharge in the model domain is primarily influenced by land slope, precipitation, drainage density, and lineament density. To identify potential groundwater recharge zones, the analytic hierarchy process (AHP) multi-criteria decision making (MCDM) technique proposed by Ponnusamy et al. (2022) was used. This technique assimilated four thematic layers—including slope, rainfall, drainage density, and lineament density—with each layer assigned a subjective relative weight under the AHP-MCDM technique (Table 1). To assess the significance and relative importance of each factor, weights were assigned accordingly. A lower value indicates relatively lower importance compared to other thematic layers, while a higher value indicates greater importance. To ensure consistency in the weights assigned to different thematic layers and their subclasses, a consistency ratio was computed. The results demonstrated that the normalized weights were consistent, as supported by a consistency ratio of 0.05, falling within the acceptable range (Saaty 2001). The thematic layers were then overlaid in ArcGIS Pro to identify potential groundwater recharge zones. Based on

**Table 1** Classification of weighting factor influencing the groundwater potential recharge zones

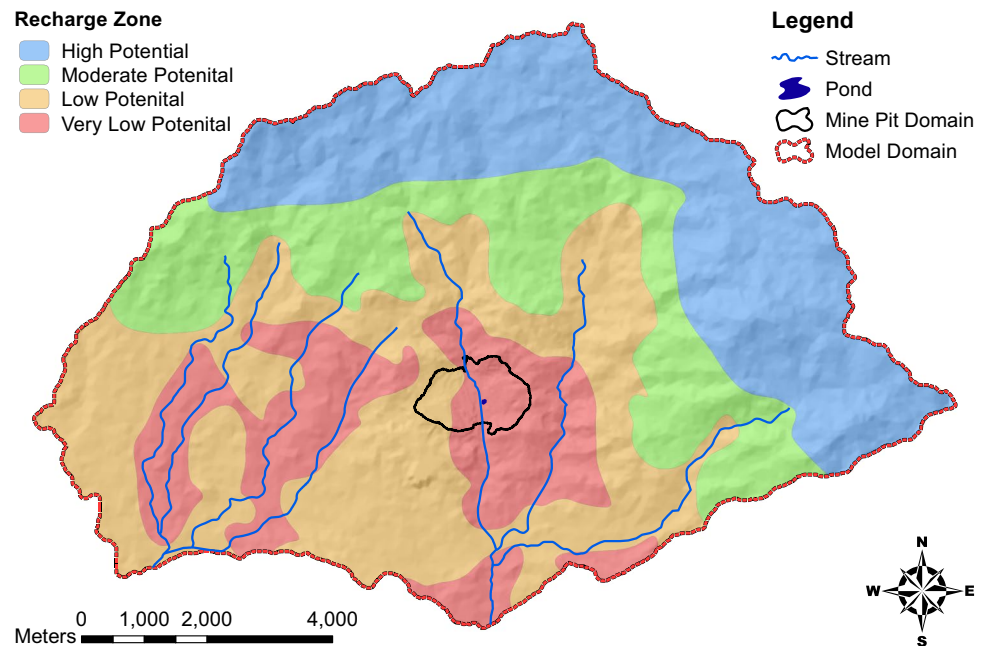
Thematic layer	% Influencing factor	No. of features	Weight factor
Precipitation (mm)	48	224–275	17
		275–327	30
		327–378	53
Slope (degree)	34	0–2	45
		2–8	31
		8–15	12
		15–30	8
		> 30	4
Drainage density (km <sup>-1</sup> )	13	0–1	50
		1–2	31
		2–3	9
		3–4	6
		> 4	4
Lineament density (km <sup>-1</sup> )	5	0–1.5	3
		1.5–3	13
		3–4.5	21
		4.5–6	29
		> 6	34

the analysis, the model domain was divided into four potential groundwater recharge zones, classified as high, moderate, low, and very low, based on their potential to recharge from precipitation (Fig. 8).

The average groundwater recharge ratio in the hydrological basins, which encompass the study area, is ~13.4% of the total annual precipitation (Noori et al. 2023). Furthermore, based on water budget computations carried out by SRK (2018), the study area experiences an average groundwater recharge rate that amounts to 10–15% of the total annual precipitation. Recharge rates from precipitation were estimated



**Fig. 8** Potential groundwater recharge zones identified using the AHP-MCDM technique



for each potential zone during the steady-state modeling period, with values ranging from 0.16 mm/day for regions with very low potential to 0.26 mm/day for regions with high potential.

### Defining the progressive open pit mine

To model the impacts of the Dareh-Zar mine excavation on the surrounding groundwater system, the finite-element grid was manipulated by collapsing specific elements and their corresponding nodes at discrete time steps. This process involved reducing the elevation of these elements to match the planned pit bottom elevation while maintaining their original X and Y coordinates. Creating a mine plan in MINEDW is often achieved by importing DXF files depicting the pit topography at various points in time. These DXF files are initially transformed into data files containing X, Y, and Z coordinates of the pit surface. These coordinates are then interpolated to construct a time-dependent mine plan. The resulting mining input file is fed into MINEDW, which simulates the progressive excavation of the open pit mine over time. It is important to note that the Dareh-Zar 3D ore body model was developed by simulating information obtained from 228 boreholes with a total drilling length of 89.1 km using the ordinary kriging method (Keyvanian et al. 2007), in addition to geological studies. Utilizing this model and data on the slope of the mine walls, specifically a minimum slope of 32° in the western region and maximum slope of 40° in the southern and eastern areas, along with a yearly mineral extraction capacity of 10.8 million tons (10,800,000 kg), an optimization of the extraction plans for

a 17-year period (from January 2023 to January 2040) was performed. This optimization was achieved by employing the NPV Scheduler software within the Datamine software environment. The NPV Scheduler is a management tool designed to optimize open pit mine production schedules with the goal of maximizing the net present value (NPV), a critical financial metric for mine profitability (Asad and Topal 2011). This tool facilitates the determination of the optimal sequence of mining blocks, considering various constraints and objectives. Ultimately, through the utilization of extraction plans, the depth and lateral advancement of the Dareh-Zar open pit was determined for over 204 monthly timesteps within the groundwater model.

### Zone of relaxation

Mining activities often cause changes in the mechanical properties of bedrock by releasing stress through the removal of overburden and blasting. These alterations typically result in increased hydraulic conductivity and porosity due to the increased density and aperture of fractures (Chen et al. 2015). The magnitude of this increase in hydraulic conductivity can vary depending on the specific rock properties and mining techniques employed. In larger open pits, where mine wall heights exceed 15 m, the zone affected by blast damage may extend more than 40 m beyond the wall (Read and Stacey 2009). It is generally agreed that the combination of removal of overburden and blast damage can increase permeability by up to three orders of magnitude, although the ratio of increase may be even greater in unaltered, brittle rock types (Aoyagi et al. 2017). The impact of mining

activities on hydraulic conductivity within the ZOR can be represented by the following equation (Itasca Denver 2018):

$$K_{zj} = \alpha_j K_{0j} \quad (1)$$

where  $K_{zj}$  is the hydraulic conductivity of unit  $j$  in the zone of relaxation (ZOR) [ $L^1T^{-1}$ ],  $\alpha_j$  is the scaling factor for unit  $j$  in the ZOR [ $L^0$ ], and  $K_{0j}$  is the initial hydraulic conductivity of unit  $j$  [ $L^1T^{-1}$ ].

In the current study, the ZOR was characterized as a region with a thickness equivalent to one-third of the pit depth, and divided into two distinct layers. Thus, the thickness of ZOR is minimal at the periphery of the pit and progressively increased towards its central region.

### Calibration and validation

The model was calibrated to groundwater level data obtained from 20 boreholes located within the model domain in both steady-state (March 2017) and transient (2017–2021) conditions. Specifically, the calibration process involved designating the groundwater level data as calibration targets and iteratively adjusting the hydraulic conductivity and areal recharge values to meet the acceptable error thresholds during steady-state simulation. To achieve this, the difference between simulated and observed water-table elevations converged within a range of less than 2% of the observed water-table elevation changes within the study area during steady-state simulation. Furthermore, specific storage values were calibrated using the trial-and-error approach, based on the estimated specific storage margin values from the pumping test and WTF method during transient calibration. The calibrated hydraulic conductivity of various HSUs within the surficial layers of the groundwater model ranges from 0.08 to 0.12 m/day. These values are consistent with documented

hydraulic conductivity variations in fractured and igneous metamorphic rocks (Atkinson 2000). Igneous rocks, characterized by a wide range of grain sizes such as pyroclastic breccias, typically exhibit higher hydraulic conductivities compared to rocks with a more uniform grain size distribution, such as basalts (Assaad and LaMoreaux 2004). Consequently, the hydraulic conductivity in the northern section of the model domain, primarily composed of andesitic basalt, demonstrates a smaller value compared to the southwestern region, predominantly consisting of andesitic breccia. However, in the central part of the model domain, where the fracture network is more extensive due to higher fault density, this value has been increased (Fig. 9). Additionally, in the southern segment of the model domain, comprising volcano-sedimentary complex and agglomerate tuff formations, there is a slight reduction in hydraulic conductivity values. This decline could be attributed to diagenesis processes and the formation of cements (Jackson and Fenelon 2022). At greater depths, hydraulic conductivity values decrease to less than 0.01 m/day (Shahbazi et al. 2020). This decline may be attributed to compaction, which reduces pore and fracture sizes; furthermore, as depth increases, the geothermal gradient encourages mineral recrystallization, filling pore spaces and fractures, ultimately reducing hydraulic conductivity (Luc Leroy et al. 2021). In the open pit mine, where mining operations have reduced the rock mass quality, and along faults and crushed zones, hydraulic conductivity values range from 1.6 to 3.1 m/day. This range is consistent with hydraulic conductivity changes observed in field hydraulic conductivity tests (SRK 2018). The distribution of calibrated hydraulic conductivity values is depicted in Fig. 9. The calibrated specific storage values exhibit a range from  $2 \times 10^{-6}$  within various lithostratigraphic units to  $6 \times 10^{-6}$  within crushed zones. The Dareh-Zar groundwater model simulation period spans from April 2017 to

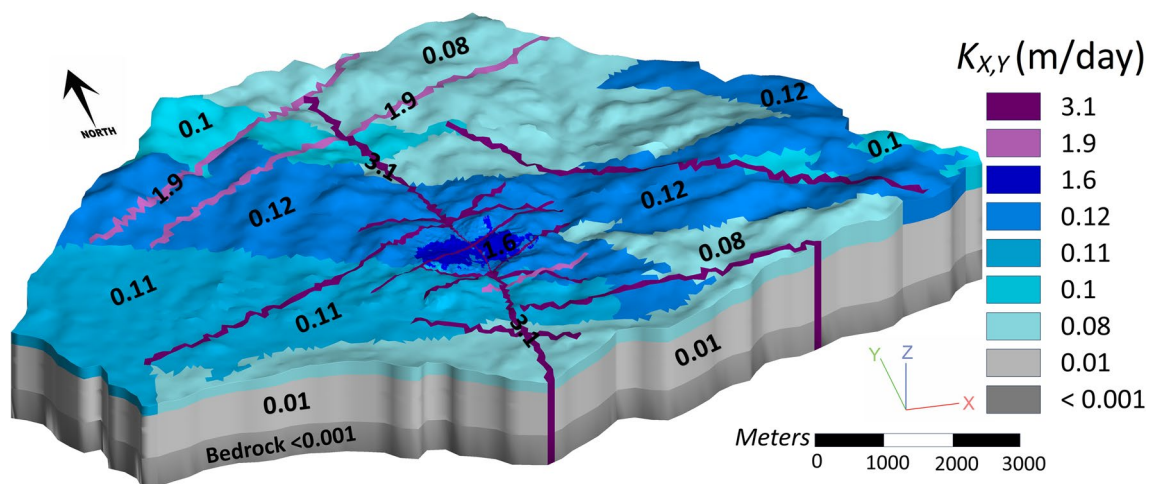


Fig. 9 Distribution of calibrated hydraulic conductivity values

April 2045, using monthly time steps. The simulation period covers 28 years, which is divided into 336 monthly time steps. The model was calibrated for the first 4 years under transient state conditions, and the proceeding 19 years were used for predictive modeling and scenario analysis, and the final 5 years for mine closure.

### Groundwater management strategies for mine closure

Post-closure, two groundwater management scenarios for the remaining open pit excavation are available: (1) no backfill, where the pit is allowed to become a lake, and (2) backfilling with appropriate materials, which prevents lake formation and maintains a passive hydraulic sink (Johnson and Carroll 2007). In the following sections, these two scenarios will be simulated and evaluated.

#### Lake scenario

To simulate the formation of the Dareh-Zar pit lake, the MINEDW Pit Lake package was utilized. To accomplish this, the drain nodes positioned on the surface of the Dareh-Zar open pit were transformed into lake nodes, and their heads were determined based on the predicted elevation of the pit lake surface. The detailed procedure for calculating the discharge into or out of the pit lake is provided in the [Appendix](#). The major components of a pit lake water budget include groundwater, direct rainfall into the pit, evaporation, and surface runoff (pit wall runoff; Tuheteru et al. 2021). In the Dareh-Zar mine, surface runoff is prevented from entering the pit lake by a diversion canal. Therefore, the primary sources of water that enter the lake are groundwater inflows and precipitation. Evaporation from the lake surface represents the main outflow component. The estimated values of precipitation and evaporation from the free surface of water in the Dareh-Zar mine pit area are 312 and 2,317 mm/year, respectively (KMP 2019). To incorporate the impact of direct rainfall on pit lake formation in the Dareh-Zar mine, the quantity of direct precipitation in the open pit region has been deducted from the evaporation rate during the simulation. Accordingly, the simulation assumes that the evaporation rate is 2,005 mm/year.

#### Backfill scenario

Open pit mine lakes have the potential to introduce contaminants into groundwater, surface water, and the surrounding ecosystem (McCullough and Lund 2006). Pit lakes, especially in arid regions, are susceptible to evapoconcentration, which increases the concentration of contaminants posing greater risks to humans and wildlife (Shevenell et al. 1999). One strategy to reduce exposure to pit lake contaminants involves backfilling the open pit above the water table. The

MINEDW Backfilling package was used to simulate the backfilling of the Dareh-Zar open pit mine, and the final pit topography was restored to a level of 2,485.5 m, corresponding to the average level of the Dareh-Zar riverbed at the beginning of mining operations. The hydraulic conductivity estimates of resaturated waste rock backfilled in open pits range between  $10^{-5}$  to  $10^{-1}$  m/s, with the values at the upper end of the range observed in waste rock materials with low fines content (Smith 2021). For this simulation, a hydraulic conductivity value of 10 m/day was assumed for the backfilling materials.

## Results and discussion

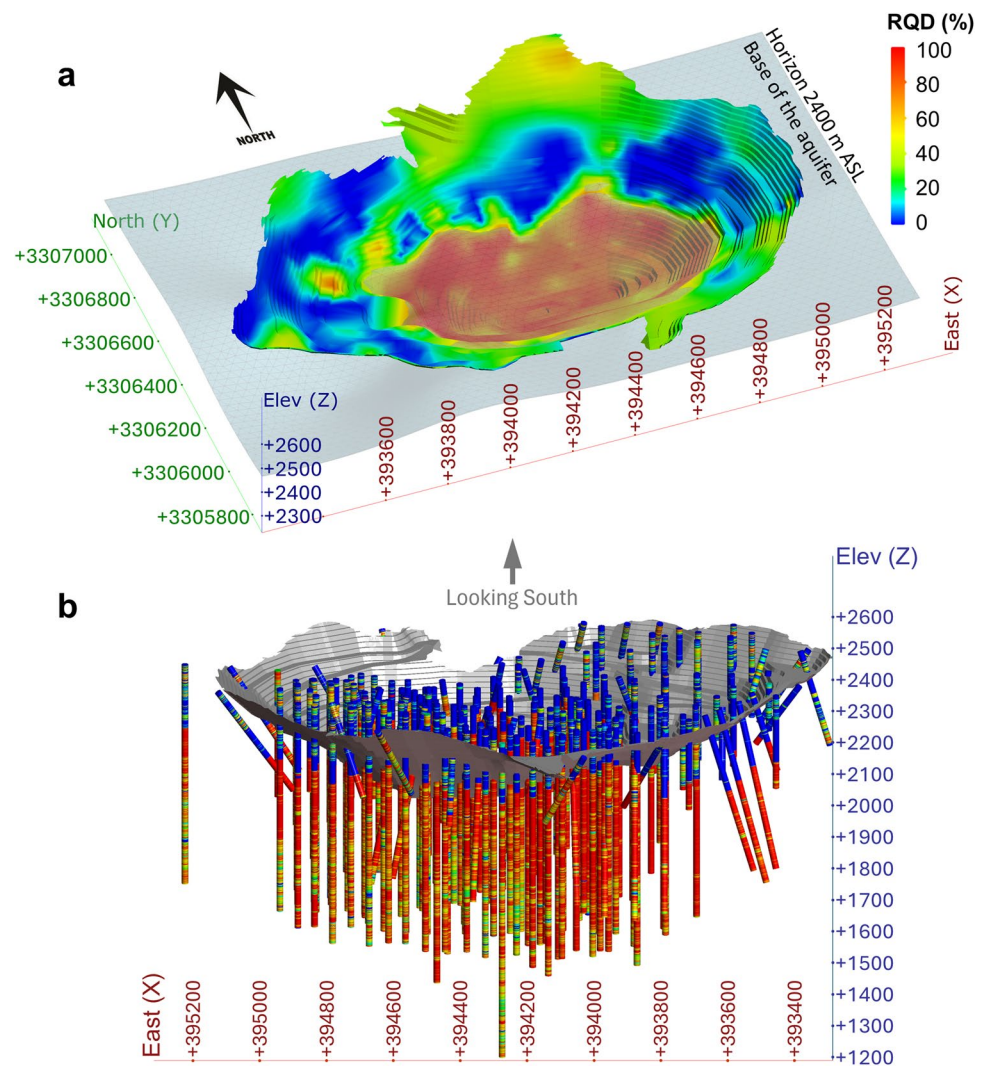
### Aquifer base

Based on the correlation analysis between rock mass permeability and the RQD data of geotechnical boreholes, as depicted in Fig. 10, discernible variation in rock mass integrity were identified in relation to depth. The results show that up to a depth of 200 m in the mine pit (2,400 m ASL), the quality of the rock mass is poor ( $25\% < \text{RQD} < 50\%$ ) or very poor ( $\text{RQD} < 25\%$ ) according to the RQD classification proposed by Deere (1988). However, below this depth, there is a significant increase in rock mass quality, ranging from good ( $75\% < \text{RQD} < 90\%$ ) to excellent ( $90\% < \text{RQD} < 100\%$ ), down to ~370 m below ground level (equivalent to the final depth of the mine pit at 2,230 m ASL). These findings led to the identification of the base of the aquifer at a depth of 2,400 m, and the model was subsequently divided into three layers.

### Model performance evaluation

The calibration of the groundwater flow model in steady-state conditions was achieved through minimizing three commonly used statistical criteria, namely the mean error (ME), absolute mean error (AME), and root mean squared error (RMSE). The calibration results are presented in Fig. 11. Additionally, model validation was conducted by comparing the simulated groundwater level hydrographs to observations. Model calibration was performed from April 2017 to January 2022 across 57 stress periods to ensure robust model performance. The comparison, depicted in Fig. 12, indicates that while the simulated hydrographs may exhibit minor deviations from observations, the overall trends are consistent. While successful calibration of a model is an essential step in simulating the behavior of an aquifer, it is important to recognize that it does not necessarily imply that the model accurately represents the actual environmental conditions (Genetti 1999). Therefore, a validation process is necessary to ensure the accuracy and credibility of the calibrated model. To validate the model, a

**Fig. 10** **a** 3D representation of changes in rock quality designation (RQD) for the planned completion of the Dareh-Zar open pit mine, and **b** RQD changes in geotechnical boreholes



comparative analysis was conducted between the simulated seepage face positions and their corresponding actual locations, as well as between the estimated quantity of leakage into the open pit mine and the observed values thereof. This process involved identifying seepage faces on Google Earth maps and comparing them with simulated seepage faces. The comparison was assessed visually as shown in Fig. 13, revealing that the location of the simulated seepage faces in the mine overlapped significantly with the observed seepage faces, particularly in the northern part of the pit. Additionally, the water budget of the model indicated that the estimated amount of seepage into the Dareh-Zar open pit mine was  $\sim 5$  L/S, which was similar to the changes in the baseflow of the Dareh-Zar River in the mining area (6 L/s). The Dareh-Zar River is significantly influenced by groundwater discharge, particularly in catchment outlets along the southern boundaries and in the central model domain, where open pit mine excavation substantially enhances the discharge process, leading to increased flow into the river.

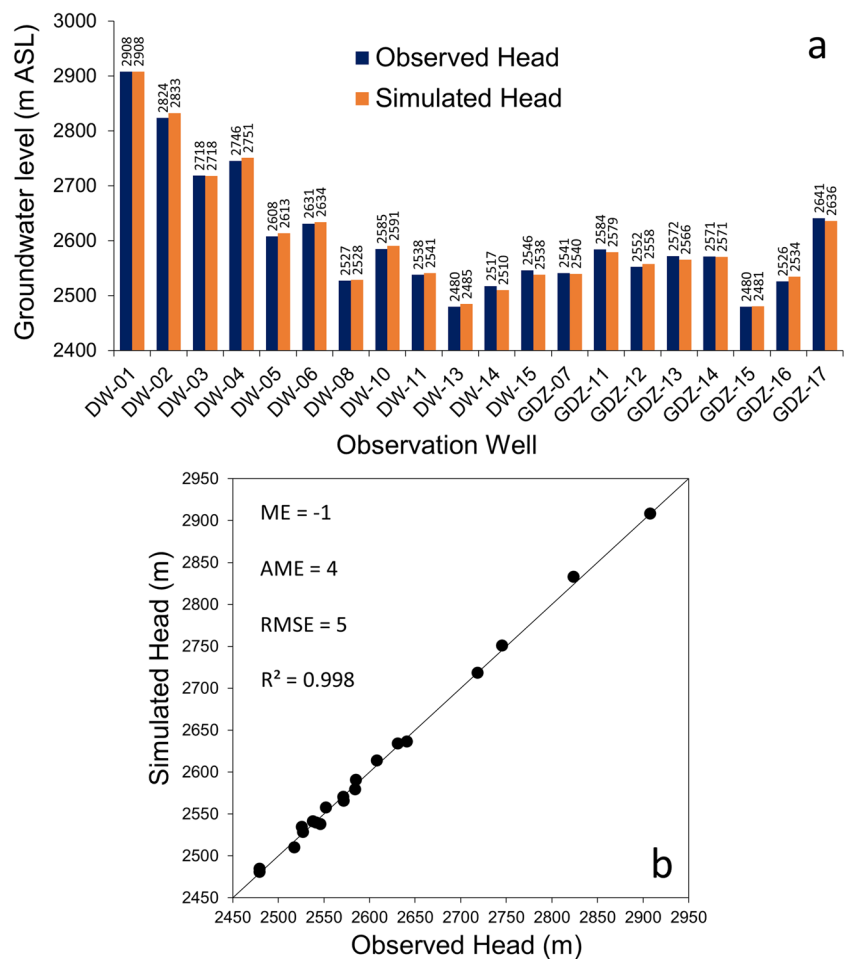
### Management scenarios analysis

Groundwater inflow rate and associated pore pressure distribution along the mine walls in the Dareh-Zar open-pit mine was evaluated using a groundwater model in three distinct scenarios, including (1) the continuation of the open pit mine excavation without the implementation of drainage management measures until mine closure (baseline scenario), (2) implementation of mine drainage through installation and operation of abstraction wells, and (3) a combination of abstraction wells and horizontal drains.

### Groundwater inflow and drainage analysis

The variation of groundwater inflow rate into the Dareh-Zar open pit mine until its closure was assessed by comparing the different drainage management scenarios (as depicted in Fig. 14). Based on the trend directions, it can be inferred that the groundwater inflow rate into the open pit mine is

**Fig. 11** **a** Bar chart comparing simulated and observed heads, and **b** scatter plot illustrating the correlation between simulated and observed heads under steady-state conditions



a function of both its excavation. In the absence of drainage measures, it is anticipated that the groundwater inflow into the open pit mine will experience a substantial increase, rising from an initial rate of  $\sim 400 \text{ m}^3/\text{day}$  to an anticipated rate of  $\sim 2,500 \text{ m}^3/\text{day}$  during the final stages of excavation. The dimensions of the final pit, after completion of mining operations, are  $\sim 1.9 \text{ km}$  in the east–west axis and  $1 \text{ km}$  in the north–south axis.

The simulation of abstraction pumping wells using the MINEDW Pumping Well package was conducted to evaluate their impact on groundwater inflow rate and pore pressure distribution of the mine walls, taking into account hydrogeological conditions, minimal disruption to mining operations, and a minimum well lifespan of 10 years. Simulations were conducted to optimize the installation and operation of abstraction wells, considering different inter-well distances, depths, and flow rates. Based on the results, a configuration of seven drainage wells, spaced  $500 \text{ m}$  apart and at a depth of  $200 \text{ m}$ , is proposed.

Model predictions suggest the implementation of abstraction wells will result in a reduction of groundwater inflow rate into the open pit by  $75\%$  during the first 12 years of mining

and  $50\%$  during the subsequent 5 years, relative to the baseline scenario (Fig. 14). Horizontal drainage boreholes provide more effective dewatering of mine pits relative to abstraction boreholes (Brawner 1982), particularly for depressurization of saturated and low-permeability highwalls, where the use of abstraction wells to mitigate pore pressure is not feasible (Seegmiller 2003). The drain boundary conditions and MINEDW Underground Mining and Dewatering package were used to define and simulate 31 horizontal drainage boreholes in the eastern and western walls of the mine. These boreholes have lengths ranging from  $70$  to  $100 \text{ m}$  and are spaced at  $50\text{-m}$  intervals. The simulation results indicate that the adoption of horizontal drains during the last 5 years of the mining operation would result in a significant reduction of  $\sim 35\%$  in the inflow of groundwater into the mine pit compared to relying exclusively on abstraction wells for drainage (Fig. 14).

### Pore pressure analysis

Determination of pore pressure distribution is a crucial parameter in slope stability assessment of the mine walls under the aforementioned scenarios. The simulation results

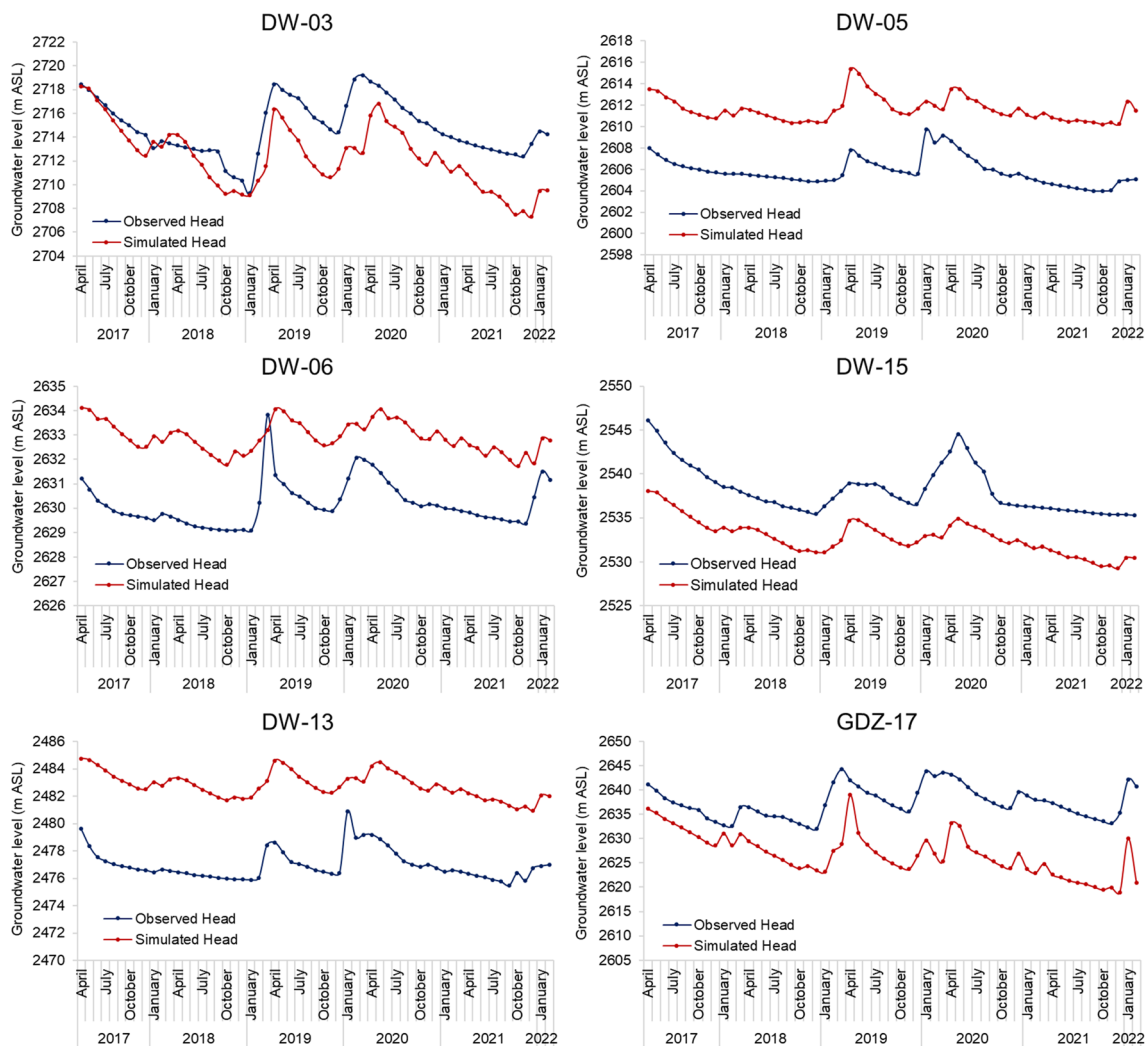


**Fig. 12** Comparison of simulated and observed groundwater levels for selected piezometers during the transient-state calibration period (2017–2022)

indicate that as the mining operation progresses and the height of the mine walls increases, particularly in the eastern and western regions of the open pit mine, the pore pressure exhibits a significant increase. Figure 15 illustrates the east–west cross-sectional profile of the pore pressure distribution in the mine pit under the mentioned scenarios, at the final timestep of the groundwater flow simulation. The findings of the model demonstrate that the implementation of an abstraction well network results in a decrease in pore pressure within the highwalls of the mine; however, during the final 5 years of mining operations, the installation of horizontal drains is required to achieve an effective reduction in pore pressure and stabilize the highwalls. The results of the model further indicate that the incorporation of horizontal drainage boreholes has a considerable impact on the depressurization of the highwalls. Figure 16 shows a 3D view of the trend of decreasing pore pressure changes

under the aforementioned drainage scenarios compared to the baseline scenario.

### Mine closure

The findings from the simulation analysis of the formation of the Dareh-Zar pit lake indicate that the pit lake dimensions progressively increase over time following mine closure. The estimated depth of the lake is projected to reach 30 m within the first 5 years post-mining. A graphical representation of the evolution and growth of the Dareh-Zar pit lake, spanning from the commencement of 2040 to the termination of 2045, is depicted in Fig. 17. Furthermore, the simulation of the open pit mine backfill scenario indicates that the surrounding water table will increase from 2,238 to 2,442 m after a 5-year backfilling process. Specifically, the simulation estimates a net restoration of ~204 m in the water table (Fig. 18).

**Fig. 13** Comparison of the locations of observed seepage faces (a), map sourced from Google Earth, with simulated seepage faces (b) in the Dareh-Zar open pit mine

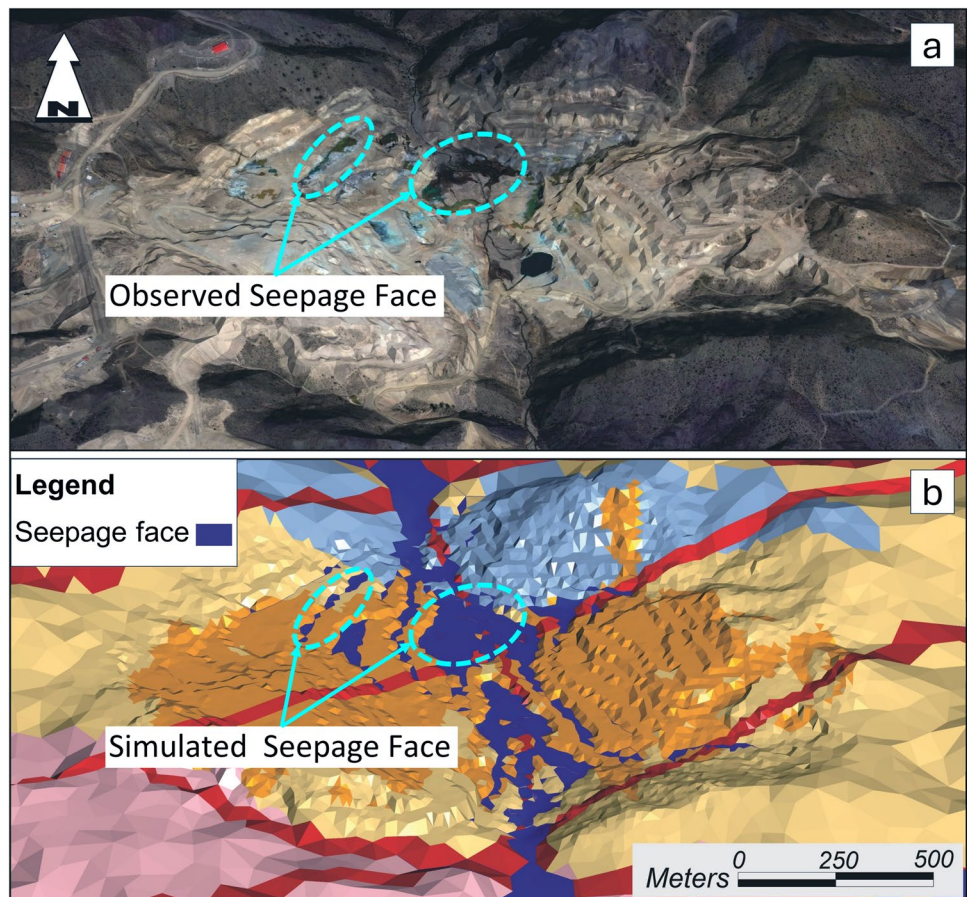
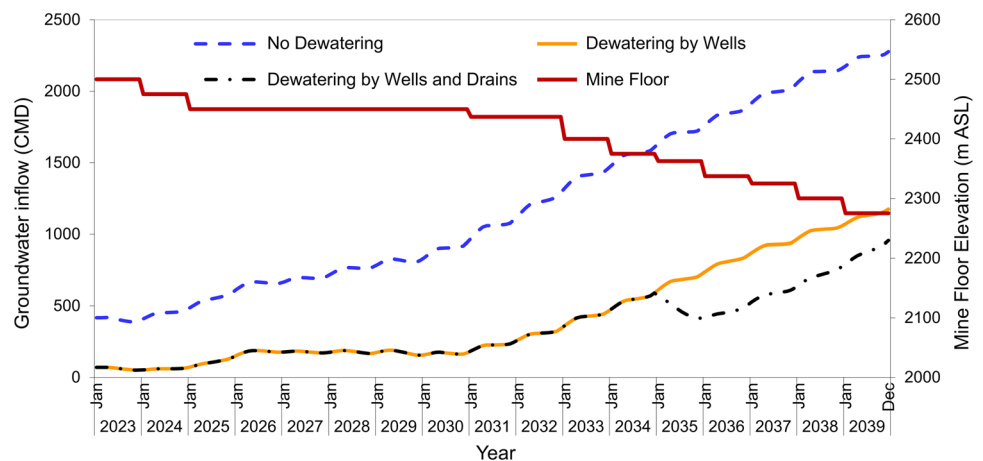


**Fig. 14** Comparison of groundwater inflow rates (CMD: cubic meters per day) in the three drainage management scenarios in comparison to the progress of the Dareh-Zar open pit mine excavation

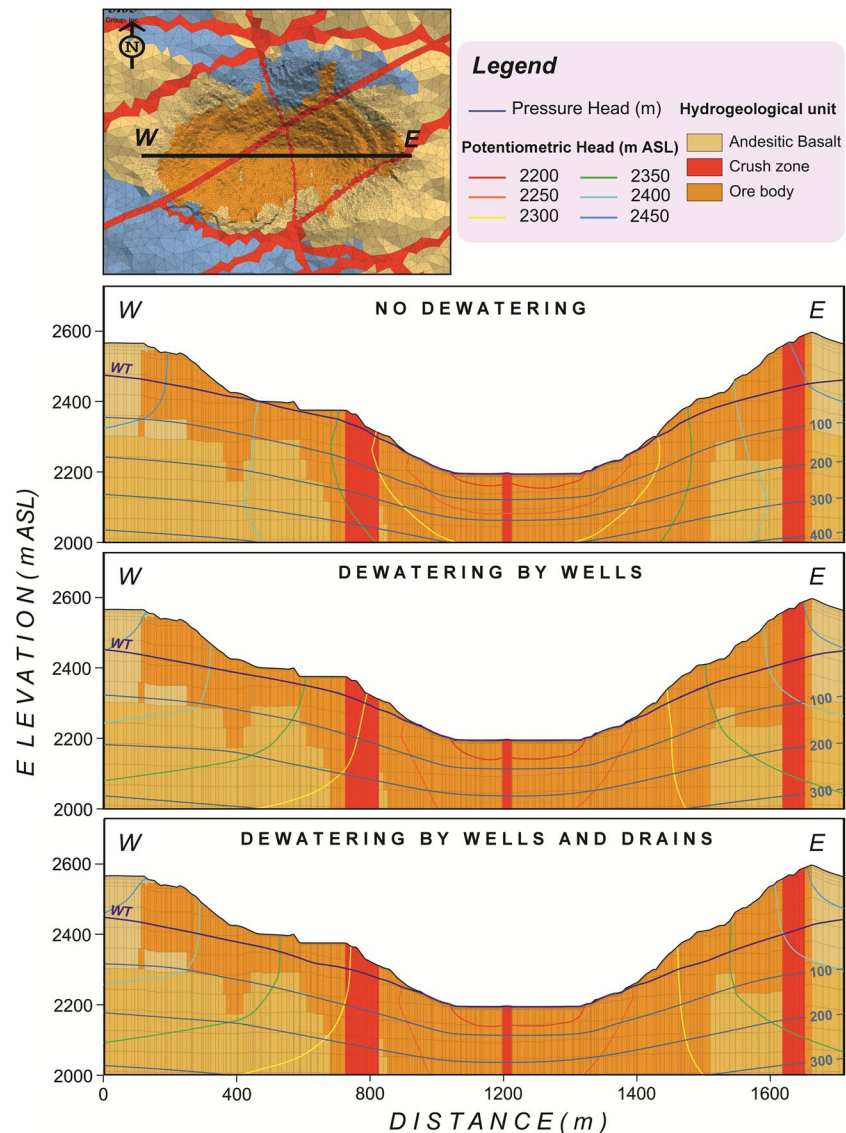


**Discussion**

Groundwater inflow rate to an open-pit mine excavation was investigated using finite element groundwater flow modeling with a dynamic mesh, considering alterations of hydraulic properties within a zone of relaxation (ZOR). The application of finite element methods and

dynamic mesh holds the potential to serve as a valuable management tool, especially in operational open pit mines with different hydrogeologic settings. This method plays a crucial role in integrating diverse data types into a coherent framework, making the information readily interpretable. The tool facilitates a rapid assessment of dewatering targets, ensuring efficient operations;

**Fig. 15** East–west cross-sectional profile of pore pressure distribution of the Dareh-Zar mine pit under different drainage scenarios predicted for December 2039



furthermore, simulating open pit development using dynamic mesh models can enhance the accuracy and efficiency of groundwater modeling in mining environments. However, the study also faces limitations—for instance, alterations in pit geometry, in addition to affecting the hydraulic properties of the rock mass surrounding the open pit, can impact various hydrogeological parameters, including the evaporation rate within the mining area. Additionally, to determine reliable boundary conditions in numerical groundwater modeling in mining environments, it is necessary to expand the model domain to include hydraulic boundaries. Consequently, the model domain primarily covers a large area. Discretizing such large-scale systems with a fine-scale mesh, especially near the model boundary and away from the pit area,

increases computational complexity and resource requirements. Conversely, using a coarse mesh may overlook locally important hydrogeological details.

Moreover, although the equivalent porous medium (EPM) approach is commonly employed for modeling fractured aquifers, it is subject to limitations in accurately simulating groundwater flow within highly heterogeneous fractured systems. The EPM's assumption of an overall hydraulic conductivity may not fully capture the significant variations in fracture distribution and hydraulic properties, particularly at smaller scales. Nonetheless, adopting a modified modeling strategy that incorporates a layered approach for significant fracture or fault zones provides a robust strategy for assessing and predicting groundwater flow in such complex aquifer systems.



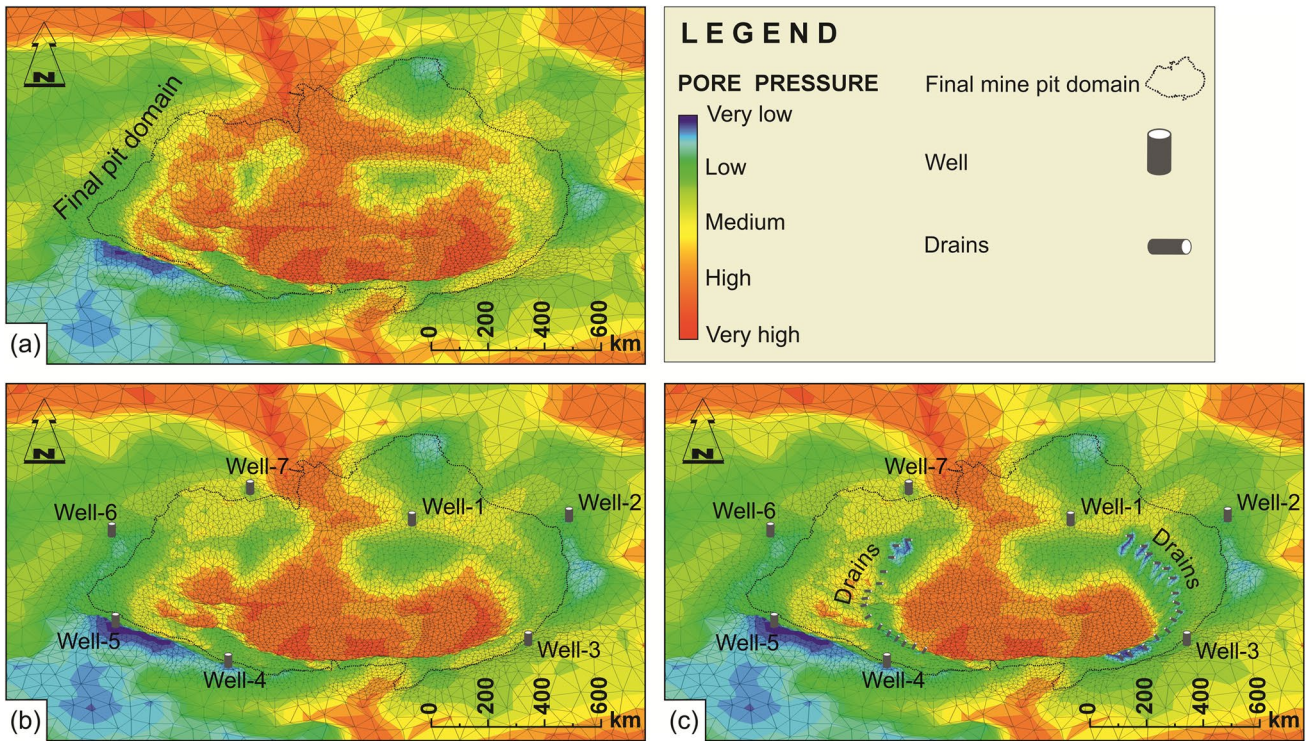


**Fig. 16** 3D view of the trend of decreasing pore pressure changes under the drainage system implementation in December 2039: (a) baseline scenario, (b) abstraction wells, and (c) combined implementation of abstraction wells and horizontal drain boreholes

**Fig. 17** Predicted Dareh-Zar open pit mine lake growth from 2040 to 2045, along with the water table for January 1, 2040

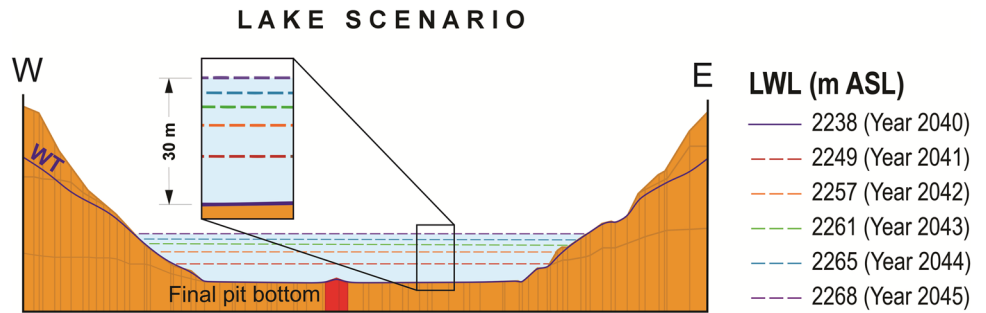
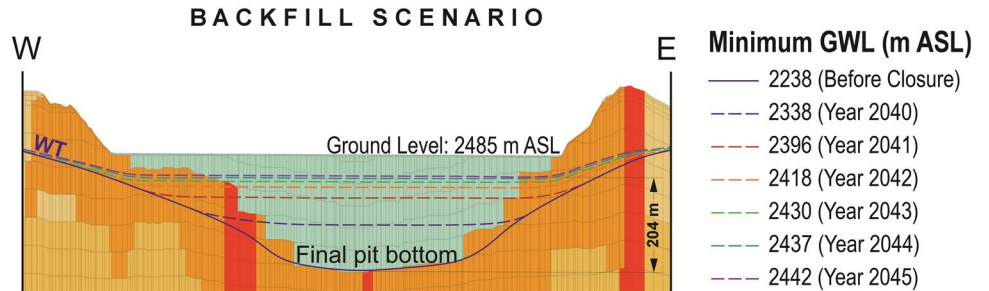


**Fig. 18** Predicted groundwater level recovery in the Dareh-Zar open pit mine following a 5-year backfilling scenario, from 2040 to 2045



## Conclusion

A numerical groundwater flow model was developed using the MINEDW code to simulate groundwater inflow rate to the Dareh-Zar open pit mine during both the mining and closure stages. The model was calibrated to observed groundwater levels and validated through comparison with observed groundwater inflows into the pit lake, confirming its reliability in simulating aquifer behavior. Model scenarios featuring the implementation of drainage measures such as abstraction wells and horizontal drains, demonstrated significant reductions in groundwater inflows to an open-pit mine excavation. Here, the simulation results of the Dareh-Zar open pit mine groundwater model demonstrated a significant reduction in groundwater inflow rate by 75% during the first 12 years of mining and 50% during the subsequent 5 years, through the adoption of abstraction wells. Incorporating horizontal drainage boreholes during the final years of mining operations further reduced groundwater inflow rate into the mine pit by ~35%, resulting in a decrease in pore pressure within the highwalls of the mine, reducing the risk of collapse.

Evaluation of open pit mine decommissioning options included pit lake and backfilling scenarios. The simulation results show that the formation of a pit lake in Dareh-Zar mine will commence immediately after mining operations cease, and its depth is projected to reach 30 m within the first 5 years post-mining. Backfilling the open pit can help prevent potential hazards associated with pit lakes, such as the introduction of contaminants into groundwater, surface water, and surrounding ecosystems. The simulation study suggests that restoring the groundwater level within the open pit mine region to ~2,442 m can be achieved through a 5-year backfilling process, representing a net restoration of ~204 m. Based on these findings, a combined approach of abstraction wells and horizontal drains is recommended for the Dareh-Zar open pit mine to ensure safe mining operations. Additionally, backfilling is recommended to mitigate potential environmental impacts associated with the pit lake.

## Appendix

Equation (2) delineates the mathematical framework used to calculate the discharge into or out of the pit lake resulting from groundwater interactions.

$$q_s = \sum_{i=1}^n \left\{ \begin{array}{l} C_{si}(H_L - H_i), \text{ if } H_{si} < H_L \\ C_{si}(H_{si} - H_i), \text{ if } H_{si} \geq H_L \text{ and } H_{si} < H_i \\ 0, \text{ if } H_{si} \geq H_L \text{ and } H_{si} \geq H_i \end{array} \right\} \quad (2)$$

where:

- $q_s$  is utilized to express the discharge to or from the pit lake [ $L^3T^{-1}$ ]
- $C_{si}$  represents the coefficient associated with node  $i$  located on the open pit surface [ $L^2T^{-1}$ ]
- $H_i$  corresponds to the computed hydraulic head at node  $i$  [L]
- $H_{si}$  represents the elevation of node  $i$  [L]
- $H_L$  is the water surface elevation of the pit lake [L]
- $n$  stands for the number of nodes [dimensionless]

Under the first condition ( $H_{si} < H_L$ ), open pit node  $i$  is beneath the pit lake surface. Discharge into the groundwater system occurs if the calculated head at the open pit node is lower than the pit lake surface elevation. Conversely, discharge exits the groundwater system when the calculated head at the open pit node exceeds the pit lake surface elevation. The second condition ( $H_{si} \geq H_L$  and  $H_{si} < H_i$ ), applies to open pit nodes above the pit lake surface. Water discharges from the groundwater system into the pit lake when the calculated head at the open pit node exceeds the node's elevation. The third condition ( $H_{si} \geq H_L$  and  $H_{si} \geq H_i$ ), pertains to open pit nodes above the pit lake with a head value lower than their respective ground surface elevations. In this situation, there is no discharge into or out of the groundwater system.

The total discharge to or from the pit lake ( $q_T$ ) consists of additional specified pumping to or from the pit lake ( $q_p$ ) and evaporation from the pit lake surface ( $q_E$ ). Equation (3) defines the mass balance relationship governing the calculation of  $q_T$ .

$$q_T = q_s + q_p - q_E \quad (3)$$

where:

- $q_T$  represents the total discharge into or out of the open pit [ $L^3T^{-1}$ ]
- $q_p$  denotes the additional pumping to or from the pit lake [ $L^3T^{-1}$ ]
- $q_E$  accounts for the discharge related to evaporation [ $L^3T^{-1}$ ]

The evaporation rate from the pit lake ( $q_E$ ) depends on the surface area of the pit lake, which varies with the pit lake elevation ( $H_L$ ) over time. The calculation of  $q_E$  is presented in Eq. (4).

$$q_E = r_E A_T \quad (4)$$

where:

- $r_E$  represents the evaporation rate from the pit lake [ $L^1T^{-1}$ ]
- $A_T$  signifies the surface area of the pit lake at time step  $t$ , functioning as a variable dependent on  $H_L$  [ $L^2$ ]

The cumulative discharge to or from the pit lake over time ( $Q$ ) is determined throughout the model run by employing the average discharge rate over the current time step ( $q_T$ ) and the preceding time step, as depicted in Eq. (5).

$$Q^t = Q^{t-1} + \frac{q_T^{t-1} + q_T^t}{2} \Delta t \quad (5)$$

where:

- $Q$  represents the cumulative discharge into the pit lake [ $L^3$ ]
- $q_T$  denotes the total discharge rate to the pit lake [ $L^3T^{-1}$ ]
- $\Delta t$  signifies the time step length [T]

## Declarations

**Conflict of interest** On behalf of all authors, the corresponding author states that there is no conflict of interest.

**Open Access** This article is licensed under a Creative Commons Attribution 4.0 International License, which permits use, sharing, adaptation, distribution and reproduction in any medium or format, as long as you give appropriate credit to the original author(s) and the source, provide a link to the Creative Commons licence, and indicate if changes were made. The images or other third party material in this article are included in the article's Creative Commons licence, unless indicated otherwise in a credit line to the material. If material is not included in the article's Creative Commons licence and your intended use is not permitted by statutory regulation or exceeds the permitted use, you will need to obtain permission directly from the copyright holder. To view a copy of this licence, visit <http://creativecommons.org/licenses/by/4.0/>.

## References

- Allen DM, Schuurman N, Deshpande A, Scibek J (2008) Data integration and standardization in cross-border hydrogeological studies: a novel approach to hydrostratigraphic model development. *Environ Geol* 53:1441–1453
- Aoyagi K, Ishii E, Ishida T (2017) Field observations and failure analysis of an excavation damaged zone in the Horonobe Underground Research Laboratory. *J MMIJ* 133:25–33
- Aryafar A, Ardejani FD, Singh R, Shokri BJ (2007) Prediction of groundwater inflow and height of the seepage face in a deep open pit mine using numerical finite element model and analytical solutions. *IMWA Symposium, Cagliari, Italy, May 2007*
- Asad MWA, Topal E (2011) Net present value maximization model for optimum cut-off grade policy of open pit mining operations. *J South Afr Inst Min Metall* 111(11):741–750
- Assaad FA, LaMoreaux PE (2004) *Field methods for geologists and hydrogeologists*. Springer, Heidelberg, Germany
- Atkinson L, Keeping P, Wright J, Liu H (2010) The challenges of dewatering at the Victor Diamond Mine in northern Ontario, Canada. *Mine Water Environ* 29:99–107
- Atkinson LC (2000) The role and mitigation of groundwater in slope stability. In: *Slope stability in surface mining*. Society for Mining, Metallurgy, and Exploration, Littleton, CO, pp 427–434
- Azrag EA, Ugorets VI, Atkinson LC (1998) Use of a finite element code to model complex mine water problems. In: *Mine water and environmental impacts*. Proc. of the International Mine Water Association Symposia, Johannesburg, South Africa, September 1998, pp 31–41
- Bahrami S, Doulati Ardejani F, Aslani S, Baafi E (2014) Numerical modelling of the groundwater inflow to an advancing open pit mine: Kolahdarvazeh pit, central Iran. *Environ Monit Assess* 186:8573–8585
- Bahrami S, Ardejani FD, Baafi E (2016) Application of artificial neural network coupled with genetic algorithm and simulated annealing to solve groundwater inflow problem to an advancing open pit mine. *J Hydrol* 536:471–484
- Barfod AA, Møller I, Christiansen AV, Høyer A-S, Hoffmann J, Straubhaar J, Caers J (2018) Hydrostratigraphic modeling using multiple-point statistics and airborne transient electromagnetic methods. *Hydrol Earth Syst Sci* 22:3351–3373
- Bense V, Gleeson T, Loveless S, Bour O, Scibek J (2013) Fault zone hydrogeology. *Earth Sci Rev* 127:171–192
- Bozan C, Wallis I, Cook PG, Dogramaci S (2022) Groundwater-level recovery following closure of open-pit mines. *Hydrogeol J* 30:1819–1832
- Brawner C (1982) Control of groundwater in surface mining. *Int J Mine Water* 1:1–16
- Cha S-S, Lee J-Y, Lee D-H, Amantini E, Lee K-K (2006) Engineering characterization of hydraulic properties in a pilot rock cavern for underground LNG storage. *Eng Geol* 84:229–243
- Chen Y-F, Zheng H-K, Wang M, Hong J-M, Zhou C-B (2015) Excavation-induced relaxation effects and hydraulic conductivity variations in the surrounding rocks of a large-scale underground powerhouse cavern system. *Tunn Undergr Space Technol* 49:253–267
- Colombo L, Gattinoni P, Scesi L (2017) Influence of underground structures and infrastructures on the groundwater level in the urban area of Milan, Italy. *Int J Sustain Dev Plan* 12:176–184
- Cotesta L, Xiang J, Paudel B, Sterrett R, Sjöberg J, Dilov T, Vasilev I, Yalamov Z (2020) Advanced three-dimensional geomechanical and hydrogeological modelling for a deep open pit. *Slope Stability* 2020:1383–1398
- Davidson S (2021) Grasshopper, algorithmic modeling for Rhino. <https://www.grasshopper3d.com/>. Accessed 11 Dec 2021
- Deere D (1988) The rock quality designation (RQD) index in practice. In: *Rock classification systems for engineering purposes*. ASTM International, West Conshohocken, PA
- Dewandel B, Alazard M, Lachassagne P, Bailly-Comte V, Couëffé R, Grataloup S, Ladouche B, Lanini S, Maréchal J-C, Wyns R (2017) Respective roles of the weathering profile and the tectonic fractures in the structure and functioning of crystalline thermomineral carbo-gaseous aquifers. *J Hydrol* 547:690–707
- Diersch H-JG (2013) *FEFLOW: finite element modeling of flow, mass and heat transport in porous and fractured media*. Springer, Heidelberg, Germany
- Durbin TJ, Bond LD (1998) *FEMFLOW3D: A finite-element program for the simulation of three-dimensional aquifers: Version 1.0*. US Geological Survey, Reston, VA
- El-Naqa A (2001) The hydraulic conductivity of the fractures intersecting Cambrian sandstone rock masses, central Jordan. *Environ Geol* 40:973–982
- Fernández-Álvarez JP, Álvarez-Álvarez L, Díaz-Noriega R (2016) Groundwater numerical simulation in an open pit mine in a limestone formation using MODFLOW. *Mine Water Environ* 35:145
- Folnagy AJ, Osiensky JL, Kobayashi D, Sprent KF (2013) Specific storage from sparse records of groundwater response to seismic waves. *J Hydrol* 503:22–28
- Genetti A (1999) *Engineering and design groundwater hydrology*. US Army Corps of Engineers, Washington, DC, 83 pp

- Gholizadeh H, Behrouj Peely A, Karney BW, Malekpour A (2020) Assessment of groundwater ingress to a partially pressurized water-conveyance tunnel using a conduit-flow process model: a case study in Iran. *Hydrogeol J* 28:2573–2585
- Giudici M, Margiotta S, Mazzone F, Negri S, Vassena C (2012) Modeling hydrostratigraphy and groundwater flow of a fractured and karst aquifer in a Mediterranean basin (Salento peninsula, south-eastern Italy). *Environ Earth Sci* 67:1891–1907
- Golian M, Teshnizi ES, Nakhai M (2018) Prediction of water inflow to mechanized tunnels during tunnel-boring-machine advance using numerical simulation. *Hydrogeol J* 26(8):2827–2851
- Golian M, Katibeh H, Singh VP, Ostad-Ali-Askari K, Rostami HT (2020) Prediction of tunnelling impact on flow rates of adjacent extraction water wells. *Q J Eng Geol Hydrogeol* 53:236–251
- Golian M, Abolghasemi M, Hosseini A, Abbasi M (2021) Restoring groundwater levels after tunneling: a numerical simulation approach to tunnel sealing decision-making. *Hydrogeol J* 29:1611–1628
- Harbaugh AW (2005) MODFLOW-2005, the US Geological Survey modular ground-water model: the ground-water flow process. US Geological Survey Reston, VA
- Holm EJ, Langtangen HP (1999) A method for simulating sharp fluid interfaces in groundwater flow. *Adv Water Resour* 23:83–95
- Hudon-Gagnon E, Chesnaux R, Cousineau PA, Rouleau A (2015) A hydrostratigraphic simplification approach to build 3D groundwater flow numerical models: example of a Quaternary deltaic deposit aquifer. *Environ Earth Sci* 74:4671–4683
- Itasca Denver, Inc (2018) Description of MINEDW Calculation Code. Itasca, Lakewood, CO
- Itasca Denver, Inc. (2023) MINEDW groundwater flow code for mining application in 3D. Ver. 3.06.235. Itasca, Denver, CO
- Jackson TR, Fenelon JM (2022) Relation of hydraulic conductivity to depth, alteration, and rock type in the volcanic rocks of Pahute Mesa, Nevada, USA. *Hydrogeol J* 30(8):2417–2432
- Jiang X-W, Wan L, Wang X-S, Wu X, Zhang X (2009) Estimation of rock mass deformation modulus using variations in transmissivity and RQD with depth. *Int J Rock Mech Min Sci* 46:1370–1377
- Jiang S, Kong X, Ye H, Zhou N (2013) Groundwater dewatering optimization in the Shengli No. 1 open-pit coalmine, Inner Mongolia, China. *Environ Earth Sci* 69:187–196
- Johnson B, Carroll K (2007) Waste rock backfill of open pits: design, optimization, and modelling considerations Conference: mine closure. Conference Proceedings, Santiago, Chile, pp 701–708
- Keyvanian SJ, Moayyed M, Borhanzadeh F, Ravankhah A (2007) Exploratory study of modeling and reserve estimation of Dareh-Zar copper mine. Paper presented at the The 26th Conference of Geological Survey and Mineral Exploration of Iran, Urmia, Iran
- KMP (2019) Dareh-Zar copper mine meteorology report. KMP, Tehran
- KMP (2020) Dareh-Zar Copper Mine geotechnical slope stability report. KMP, Tehran
- Kolapo P, Oniyide GO, Said KO, Lawal AI, Onifade M, Munemo P (2022) An overview of slope failure in mining operations. *Mining* 2:350–384
- Kollet SJ, Maxwell RM (2008) Capturing the influence of groundwater dynamics on land surface processes using an integrated, distributed watershed model. *Water Resour Res* 44(2). <https://doi.org/10.1029/2007WR006004>
- Krásný J, Sharp JM (2007) Groundwater in fractured rocks. IAH Selected Paper Series, vol 9, CRC, Boca Raton, FL
- Kresic N, Panday S (2018) Numerical groundwater modelling in karst. *Geol Soc London Spec Publ* 466:319–330
- Kuang X, Jiao JJ, Zheng C, Cherry JA, Li H (2020) A review of specific storage in aquifers. *J Hydrol* 581:124383
- Lachassagne P, Dewandel B, Wyns R (2021) Hydrogeology of weathered crystalline/hard-rock aquifers: guidelines for the operational survey and management of their groundwater resources. *Hydrogeol J* 29:2561–2594
- Li T, Song H, Huang G, Bi Y, Li X (2014) Assessment of groundwater changing trends through the generalized large well method with confined–unconfined flow model in open-pit mine area. *Environ Earth Sci* 72:4599–4606
- Luc Leroy MN, Marius FW, François N (2021) Experimental and theoretical investigations of hard rocks at high temperature: applications in civil engineering. *Adv Civil Eng* 2021:1–21
- Mali S, Jafari H, Jahanshahi R, Bagheri R (2022) Groundwater source identification and flow model of the Dareh-Zar Copper Mine in central Iran by chemo-isotopic techniques. *Mine Water Environ* 41:921–937
- McCullough CD, Lund MA (2006) Opportunities for sustainable mining pit lakes in Australia. *Mine Water Environ* 25:220–226
- Movahednia M, Maghfouri S, Fazli N, Rastad E, Ghaderi M, González FJ (2022) Metallogeny of Manto-type Cu-(Ag) mineralization in Iran: relationship with Neo-Tethyan evolution and implications for future exploration. *Ore Geol Rev* 149:105064. <https://doi.org/10.1016/j.oregeorev.2022.105064>
- NICICO (2017) Dareh-Zar Copper Mine Topographic Map, Scale: 1/1,000. National Iranian Copper Industries Co., Tehran
- Noori R, Maghrebi M, Jessen S, Bateni SM, Heggy E, Javadi S, Agha-Kouchak A (2023) Decline in Iran's groundwater recharge. *Nat Commun* 14(1):6674
- Omajev V, Isailović S (1969) Geological map of Pariz, Scale: 1/20,000. Geological Survey and Mineral Exploration of Iran, Tehran
- Parizi HS, Samani N (2014) Environmental isotope investigation of groundwater in the Sarcheshmeh copper mine area, Iran. *Mine Water Environ* 33:97
- Piscopo V, Baiocchi A, Lotti F, Ayan EA, Biler AR, Ceyhan AH, Cüylan M, Dişli E, Kahraman S, Taşkın M (2018) Estimation of rock mass permeability using variation in hydraulic conductivity with depth: experiences in hard rocks of western Turkey. *Bull Eng Geol Env* 77:1663–1671
- Polomčić D, Bajić D (2015) Application of Groundwater modeling for designing a dewatering system: case study of the Buvač Open Cast Mine, Bosnia and Herzegovina. *Geol Croatica* 68:123–137
- Ponnusamy D, Rajmohan N, Li P, Thirumurugan M, Chidambaram S, Elumalai V (2022) Mapping of potential groundwater recharge zones: a case study of Maputland plain, South Africa. *Environ Earth Sci* 81:418
- Qureshi MU, Khan KM, Bessaih N, Al-Mawali K, Al-Sadrani K (2014) An empirical relationship between in-situ permeability and RQD of discontinuous sedimentary rocks. *Electron J Geotech Eng* 19:4781–4790
- Read J, Stacey P (2009) Guidelines for open pit slope design. CISRO, Collingswood, VIC, Australia
- Renard F (2021) Reaction-induced fracturing: when chemistry breaks docks. *J Geophys Res: Solid Earth* 126: e2020JB021451
- Rivera A (2007) Groundwater modelling: from geology to hydrogeology. Geology Survey of Canada, Quebec, QC
- Robins N, Rutter H, Dumbleton S, Peach D (2005) The role of 3D visualisation as an analytical tool preparatory to numerical modelling. *J Hydrol* 301:287–295
- Rossmann N, Zlotnik VA, Rowe C (2018) An approach to hydrogeological modeling of a large system of groundwater-fed lakes and wetlands in the Nebraska Sand Hills, USA. *Hydrogeol J* 26:8881–897
- Rózkowski K, Zdechlik R, Chudzik W (2021) Open-pit mine dewatering based on water recirculation: case study with numerical modelling. *Energies* 14:4576
- Saaty TL (2001) Decision making for leaders: the analytic hierarchy process for decisions in a complex world RWS publications. University of Pittsburgh, Pittsburgh, PA

- Sahraei Parizi H, Samani N (2013) Geochemical evolution and quality assessment of water resources in the Sarcheshmeh copper mine area (Iran) using multivariate statistical techniques. *Environ Earth Sci* 69:1699–1718
- Sashikkumar M, Selvam S, Kalyanasundaram VL, Johnny JC (2017) GIS based groundwater modeling study to assess the effect of artificial recharge: a case study from Kodaganar river basin, Dindigul district, Tamil Nadu. *J Geol Soc India* 89:57–64
- Scanlon BR, Mace RE, Barrett ME, Smith B (2003) Can we simulate regional groundwater flow in a karst system using equivalent porous media models? Case study, Barton Springs Edwards aquifer, USA. *J Hydrol* 276:137–158
- Seegmiller BL (2003) Horizontal drains: there use in open pit mine dewatering. Seegmiller Assoc., Salt Lake City, UT
- Seiler K-P, Gat JR (2007) Groundwater recharge from run-off, infiltration and percolation. Springer, Heidelberg, Germany
- Shahbazi A, Saeidi A, Chesnaux R (2020) A review of existing methods used to evaluate the hydraulic conductivity of a fractured rock mass. *Eng Geol* 265:105438
- Shapiro AM, Ladderud JA, Yager RM (2015) Interpretation of hydraulic conductivity in a fractured-rock aquifer over increasingly larger length dimensions. *Hydrogeol J* 23(7):1319
- Sharp JM (2014) Fractured rock hydrogeology. CRC, Boca Raton, FL
- Shevenell L, Connors KA, Henry CD (1999) Controls on pit lake water quality at sixteen open-pit mines in Nevada. *Appl Geochem* 14:669–687
- Smith L (2021) Hydrogeology and mineral resource development. The Groundwater Project, Guelph, ON
- SRK (2018) Sarcheshmeh Copper Mine hydrogeology report. SRK, Johannesburg, South Africa
- Surinaidu L, Rao VG, Rao NS, Srinu S (2014) Hydrogeological and groundwater modeling studies to estimate the groundwater inflows into the coal mines at different mine development stages using MODFLOW, Andhra Pradesh, India. *Water Resour Indust* 7:49–65
- Tachikawa T, Kaku M, Iwasaki A, Gesch DB, Oimoen MJ, Zhang Z, Danielson JJ, Krieger T, Curtis B, Haase J, Abrams M (2011) ASTER global digital elevation model version 2-summary of validation results. NASA, Washington, DC
- Taherkhani H, Doostmohammadi R (2015) Transportation costs: a tool for evaluating the effect of rock mass mechanical parameters on blasting results in open pit mining. *J Min Sci* 51:730–742
- Tuheteru EJ, Gautama RS, Kusuma GJ, Kuntoro AA, Pranoto K, Pallinggi Y (2021) Water balance of pit lake development in the equatorial region. *Water* 13:3106
- Ugorets V (2015) Benefits of MINEDW code for mine dewatering projects in complex hydrogeological settings. Itsaca, Lakewood, CO
- Wang Q, Chen C, Chen B, Xia J, Du J (2013) Feasibility of estimating groundwater storage changes in western Kansas using Gravity Recovery and Climate Experiment (GRACE) data. *Lead Edge* 32:806–813
- Wels C, Mackie D, Scibek J (2012) Guidelines for groundwater modeling to assess impacts of proposed natural resource development activities. Ministry of Environment, Water Protection & Sustainability Branch, Province of British Columbia, Victoria, BC
- Xu Y, Beekman HE (2019) Groundwater recharge estimation in arid and semi-arid southern Africa. *Hydrogeol J* 27:929–943
- Yang F-R, Lee C-H, Kung W-J, Yeh H-F (2009) The impact of tunneling construction on the hydrogeological environment of “Tseng-Wen Reservoir Transbasin Diversion Project” in Taiwan. *Eng Geol* 103:39–58
- Zago MM, Fries M, Ramires JEF (2020) Groundwater infiltration in a gold mine: a geoelectrical investigation model as an aid to dewatering process determination. *J Appl Geophys* 172:103909

**Publisher's Note** Springer Nature remains neutral with regard to jurisdictional claims in published maps and institutional affiliations.